NUMERICAL EVALUATION OF DIFFUSIVE AND DISPERSIVE TENSORS IN PERIODIC POROUS MEDIA

PIERRE TARDIF D'HAMONVILLE[1], ALEXANDRE ERN[1], LUC DORMIEUX[2]

[1]Laboratoire CERMICS (ENPC), 6 - 8 avenue Blaise Pascal
Cité Descartes - Champs sur Marne, F-77455 Marne la Vallée Cedex 2

[2] Laboratoire LMSGC (ENPC), 6 - 8 avenue Blaise Pascal
Cité Descartes - Champs sur Marne, F-77455 Marne la Vallée Cedex 2

Abstract

We present a method to compute diffusion and dispersion tensors for three-dimensional periodic porous media in the framework of the double scale expansion technique. Numerical simulations on cubic and centered cubic sphere networks are performed to study the quantitative impact of the pore morphology and of the flow velocity on these tensors.

1. Introduction

At the macroscopic scale, the transport of a fluid component in a porous medium is governed by advective, diffusive, and dispersive fluxes. The two latter fluxes can be formulated using a diffusion tensor and a dispersion tensor (Dormieux and Bourgeois, 2002) in the form

$$\partial_t \rho + \underline{\nabla} \cdot (\rho \underline{V} - (\underline{\underline{D}}^{\hom}_{\text{diff}} + \underline{\underline{D}}^{\hom}_{\text{disp}}) \cdot \underline{\nabla} \rho) = 0$$

where ρ denotes the concentration of the solute, $\underline{V}$ the fluid velocity, and $\underline{\underline{D}}^{\hom}_{\text{diff}}$ (resp. $\underline{\underline{D}}^{\hom}_{\text{disp}}$) the diffusion tensor (resp. the dispersion tensor). The actual value of these tensors depends on the pore geometry and on the magnitude of the advection velocity.

Using the double scale expansion technique derived by (Ene and Sanchez-Palencia, 1975) and (Sanchez-Palencia, 1980) and provided the problem is homogenizable, it is well-known (Auriault, 2005) that the diffusion and dispersion tensors can be evaluated from the following procedure. First, a velocity field at the pore scale is obtained by solving a Stokes-like problem. Then, this velocity field is used in a vector-valued advection-diffusion equation, still posed at the pore scale, and from which solution the diffusion and dispersion tensors are evaluated.

Since we are interested in 3D pore geometries for which analytical solutions are not available, we use the finite element method to approximate the pore scale velocity field and the solution of the vector-valued advection-diffusion equation. The strategy for approximating the pore scale velocity field uses mixed Crouzeix-Raviart/$\mathbb{P}_0$ finite elements. Then the velocity field is projected onto a vector space of divergence-free fields using Brezzi-Douglas-Marini finite elements.

We perform numerical simulations for cubic and centered cubic networks of spheres. We also vary the velocity magnitude to study its effect on the diffusion and dispersion tensors.

2. Physical models

2.1. **Notation.** The main notation used in this article is the following :

- $\underline{y} \in \mathbb{R}^3$: space variable;
- M : macroscopic structure with periodic geometry;
- L : characteristic size of M;
- $\Omega = \{0 \leq y_i \leq a_i\}_{i=1,d}$: elementary cell of M, $(a_i \in \mathbb{R}^+ \quad \forall i \in [\![1,3]\!])$;
- ℓ : characteristic size of Ω, $(a_i \approx \ell \quad \forall i \in [\![1,3]\!])$;
- $\delta = \frac{\ell}{L} \ll 1$: parameter characterizing the separation of macroscopic and microscopic scales;
- Ω_f : fluid phase domain of Ω;
- Ω_s : solid phase domain of Ω;
- $\partial\Omega$, $\partial\Omega_\mathrm{f}$, $\partial\Omega_\mathrm{s}$: boundaries of the elementary cell, of the fluid domain and of the solid domain;
- $\partial\Omega_\mathrm{fs} = \partial\Omega_\mathrm{f} \cap \partial\Omega_\mathrm{s}$: solid-fluid interface;
- $\partial\Omega_\mathrm{ff} = \partial\Omega_\mathrm{f} \cap \partial\Omega_\mathrm{fs}$: fluid-fluid interface;
- $\underline{x}$, $\underline{z}$: space variables used in the double scale expansion technique, where $\underline{y} = (\underline{x};\underline{z})$, $\underline{x}$ is related to the dependence of the physical quantities on the macroscopic scale, and $\underline{z}$ is related to their fluctuation at the microscopic scale;
- $\underline{\nabla}_y$, $\underline{\nabla}_x$, $\underline{\nabla}_z$: gradient operators taken with respect to the original, the macroscopic, and the microscopic spatial coordinates;
- $\varphi = \frac{|\Omega_\mathrm{f}|}{|\Omega|}$: porosity of the medium;
- $\overline{a}^\mathrm{f}(\underline{x}) = \frac{1}{|\Omega_\mathrm{f}|}\int_{\Omega_\mathrm{f}} a(\underline{x},\underline{z})d\underline{z}$: intrinsic mean;
- $< a >_\mathrm{f} (\underline{x}) = \varphi\overline{a}^\mathrm{f}(\underline{x})$: apparent mean;
- $\tilde{a}(\underline{x},\underline{z}) = a(\underline{x},\underline{z}) - \overline{a}^\mathrm{f}(\underline{x})$: fluctuation of the physical quantity a;
- $a^{'}$: non-dimensional version of a;
- $a_i(\underline{x},\underline{z})$: i$^{\text{th}}$ term of the expansion of a with respect to the parameter δ, $(a(\underline{x},\underline{z}) = \sum \delta^i a_i(\underline{x},\underline{z}))$.

2.2. **Stokes problem.** The magnitude of the velocity is assumed to be small enough so that the flow at the pore scale is governed by the Stokes equations in the form

$$\begin{cases} -\mu\Delta_y\underline{u} + \underline{\nabla}_y p = \underline{0} \\ \underline{\nabla}_y \cdot \underline{u} = 0 \end{cases} \tag{1}$$

where μ denotes the fluid viscosity, $\underline{u}$ the velocity and p the pressure. At the first order, the expansion of p reads

$$p(\underline{x},\underline{z}) = p_0(\underline{x},\underline{z}) + \delta p_1(\underline{x},\underline{z}).$$

It can be shown that p_0 does not depend on $\underline{z}$. Consequently p_1 may be chosen such that $\overline{p_1}^\mathrm{f} = 0$. We introduce the macroscopic pressure gradient $\underline{\alpha} = \underline{\nabla}_x p_0$. We denote by α the Euclidean norm of $\underline{\alpha}$ and we set $\underline{e}_\alpha = \frac{1}{\alpha}\underline{\alpha}$. Using the non-dimensional quantities $\underline{x}^{'} = \frac{1}{L}\underline{x}$

and $\underline{z}^{'} = \frac{1}{\ell}\underline{z}$ leads to the following non-dimensional problem

$$\begin{cases} -\Delta_{z'}\underline{u}^{'} + \underline{\nabla}_{z'} p_1^{'} = -\underline{e}_\alpha & (\Omega'_{\rm f}) \\ \underline{\nabla}_{z'} \cdot \underline{u}^{'} = 0 & (\Omega'_{\rm f}) \\ \underline{u}^{'} = 0 \quad \text{on } (\partial\Omega'_{\rm fs}) \quad ; \quad \underline{u}^{'}, p_1^{'} \text{ periodic on } (\partial\Omega'_{\rm ff}) \end{cases} \tag{2}$$

where $\underline{u}^{'} = \frac{\mu}{\ell^2\alpha}\underline{u}$, $p_1^{'} = \frac{1}{\alpha L}p_1$, $\Omega'_{\rm f} = \{\underline{z}^{'}; \ell\underline{z}^{'} \in \Omega_{\rm f}\}$, and $\partial\Omega'_{\rm fs}$ and $\partial\Omega'_{\rm ff}$ are defined similarly.

The velocity scale is $U_{\rm f} = \varsigma_{\Omega'_{\rm f}} \frac{\alpha\ell^2}{\mu}$ where $\varsigma_{\Omega'_{\rm f}}$ is a non-dimensional parameter (depending only on the pore morphology) which is equal to the maximum value of the Euclidean norm of $\underline{u}^{'}$. The Reynolds number can be evaluated as $Re = \varsigma_{\Omega'_{\rm f}} \frac{\rho_w \alpha \ell^3}{\mu^2}$ where ρ_w denotes the mass density of the fluid, and the validity of the Stokes model for the fluid flow amounts to $Re \leq 1$. This inequality yields an upper bound for the magnitude of the macroscopic pressure gradient α.

2.3. **Advection-diffusion problem.** The model that describes the solute transport at the microscopic scale is an advection-diffusion equation expressing the mass balance of the solute using Fick's law for the diffusive flux. On the boundary $\partial\Omega_{\rm fs}$ there is no exchange between the solid and the fluid phases. The problem reads

$$\begin{cases} \partial_t \rho + \underline{\nabla}_y \cdot \left(\rho\underline{u} - D\underline{\nabla}_y \rho\right) = 0 & (\Omega_{\rm f}) \\ \underline{\nabla}_y \rho \cdot \underline{n} = 0 & (\partial\Omega_{\rm fs}) \end{cases} \tag{3}$$

where ρ denotes the concentration of the solute, D the diffusion coefficient associated with Fick's law, and $\underline{n}$ the unit outward normal to $\partial\Omega_{\rm fs}$.

It is convenient to introduce the reference velocity $U_D = \frac{D}{L}$. We focus on the advection dominated regime in which $U_{\rm f} \approx \delta^{-1} U_D$ and we assume that the time scale of advection is of the same order of the time scale of concentration changes. The latter hypothesis makes the transient term negligible in the asymptotic analysis. Introducing the non-dimensional velocity $\underline{u}^* = \delta U_D^{-1}\underline{u}$ and using the non-dimensional form of the problem and the double scale expansion technique, it can be shown that $\rho_0^{'}$ only depends on the macroscopic variable $\underline{x}^{'}$. So $\rho_1^{'}$ can be chosen such that $\overline{\rho_1^{'}}^{\rm f} = 0$ and $\underline{\nabla}_{x'}\rho_0^{'}$ is the macroscopic concentration gradient. It plays the role of the source term in the microscopic problem. We observe that $\rho_1^{'}$ depends linearly on $\underline{\nabla}_{x'}\rho_0^{'}$. Consequently there exists a vector field $\underline{\chi}$ such that $\rho_1^{'} = \underline{\chi} \cdot \underline{\nabla}_{x'}\rho_0^{'}$ and $\underline{\chi}$ solves the non-dimensional problem

$$\begin{cases} -\Delta_{z'}\underline{\chi} + \underline{\underline{\nabla}}_{z'}\chi \cdot \underline{u}^* = \overline{\underline{u}^*}^{\rm f} - \underline{u}^* & (\Omega'_{\rm f}) \\ {}^t\underline{\underline{\nabla}}_{z'}\chi \cdot \underline{n} = -\underline{n} & (\partial\Omega'_{\rm fs}) \end{cases} \tag{4}$$

Switching back to dimensional quantities, the diffusive flux reads (Bear and Bachmat, 1990)

$$\underline{j} = D(\underline{\underline{1}} + {}^t\underline{\underline{\nabla}}_{z'}\chi) \cdot \underline{\nabla}_x \rho_0 \quad \Rightarrow \quad <\underline{j}>_{\rm f} = -\varphi D(\underline{\underline{1}} + {}^t\overline{\underline{\underline{\nabla}}_{z'}\chi}^{\rm f}) \cdot \underline{\nabla}_x \rho_0$$

and the dispersive flux reads

$$\tilde{\rho}\tilde{\underline{u}} = D(\tilde{\underline{u}}^* \otimes \underline{\chi}) \cdot \underline{\nabla}_x \rho_0 \quad \Rightarrow \quad <\tilde{\rho}\tilde{\underline{u}}>_{\rm f} = -(-\varphi D\overline{\underline{u}^* \otimes \underline{\chi}}^{\rm f}) \cdot \underline{\nabla}_x \rho_0$$

In these expressions the homogenized diffusion and dispersion tensors appear clearly :

$$\underline{\underline{D}}^{\text{hom}}_{\text{diff}} = \varphi D(\underline{\underline{1}} + {}^{t}\overline{\underline{\underline{\nabla}}_{z'}\chi}^{\text{f}}) \qquad \underline{\underline{D}}^{\text{hom}}_{\text{disp}} = -\varphi D\overline{\underline{u}^{*} \otimes \underline{\chi}}^{\text{f}}$$

3. Approximation by Finite Elements

Numerical approximations using the finite element method are performed to solve the fluid flow and the advection-diffusion problems (Ern and Guermond, 2004). The numerical problems deal with non-dimensional quantities only. To alleviate the notation, the prime superscript is no longer used.

Let $\{\mathcal{T}_h\}$ a family of meshes of Ω_{f} with periodicity properties on $\partial\Omega_{\text{ff}}$. It means that the trace of $\mathcal{T}_h$ on the plane $\{z_i = \frac{a_i}{\ell}\}$ is an image by translation of the trace of $\mathcal{T}_h$ on the plane $\{z_i = 0\}$.

3.1. Approximation of the flow problem.

Let $P^1_{\text{CR},h}$ be the Crouzeix-Raviart finite element space whose functions have null mean-value on the faces of the mesh which are situated on $\partial\Omega_{\text{fs}}$ and periodicity properties on $\partial\Omega_{\text{ff}}$. Let P^0_h be the space defined as follows :

$$P^0_h = \{v_h \in L^2(\Omega_{\text{f}});\ \forall \tau \in \mathcal{T}_h\ v_h|_\tau \in P^0,\ \int_{\Omega_{\text{f}}} v_h = 0\}.$$

In the sequel, $\underline{\nabla}_h$ denotes the gradient operator localized at mesh elements without taking into account Dirac surface measures that can possibly result from discontinuities across mesh interfaces. We seek $(\underline{u}_h, p_{1h}) \in (P^1_{\text{CR},h})^3 \times P^0_h$ such that

$$\left\{ \begin{array}{ll} \displaystyle\int_{\Omega_{\text{f}}} \underline{\underline{\nabla}}_h \underline{u}_h : \underline{\underline{\nabla}}_h \underline{v}_h - \int_{\Omega_{\text{f}}} p_{1h}(\underline{\nabla}_h \cdot \underline{v}_h) + \int_{\Omega_{\text{f}}} \underline{e}_\alpha \cdot \underline{v}_h = 0 & \forall \underline{v}_h \in (P^1_{\text{CR},h})^3 \\ \displaystyle\int_{\Omega_{\text{f}}} q\, \underline{\nabla}_h \cdot \underline{u}_h = 0 & \forall q \in P^0_h. \end{array} \right. \tag{5}$$

The following error estimate is classical

$$\|\underline{u} - \underline{u}_h\|_{0,\Omega_{\text{f}}} + h\|\underline{\underline{\nabla}} u - \underline{\underline{\nabla}}_h u_h\|_{0,\Omega_{\text{f}}} + h\|p_1 - p_{1h}\|_{0,\Omega_{\text{f}}} \leq ch^2$$

where c depends on the exact solution but is independent of h.

The divergence of the discrete velocity field $\underline{u}_h$ vanishes piecewise on all the mesh cells (i.e. $\underline{\nabla}_h \cdot \underline{u}_h = 0$). However, owing to its discontinuities across the mesh faces, the discrete velocity field $\underline{u}_h$ is not conservative (i.e. divergence-free). To obtain a conservative field, a projection of $\underline{u}_h$ inspired from (Bastian and Rivière, 2003) is performed on the finite element space of Brezzi-Douglas-Marini (Brezzi, Douglas and Marini, 1985). Let $\pi_h u_h$ denote this projection. The following holds (Tardif d'Hamonville, Ern and Dormieux, 2006)

$$\underline{\nabla} \cdot (\pi_h u_h) = 0 \qquad \|\underline{u} - \pi_h \underline{u}_h\|_{0,\Omega_{\text{f}}} \leq ch^2$$

It means that the projected velocity $\pi_h \underline{u}_h$ is conservative and that the projection does not alter the accuracy of the finite element method.

	Stokes			advection-diffusion	
i	$\|\underline{u}-\underline{u}_h\|_{0,\Omega_\mathrm{f}}$	$\|\underline{u}-\underline{u}_h\|_{1,\Omega_\mathrm{f}}$	$\|\phi-\phi_h\|_{0,\Omega_\mathrm{f}}$	$\|\underline{\chi}-\underline{\chi}_h\|_{0,\Omega_\mathrm{f}}$	$\|\underline{\chi}-\underline{\chi}_h\|_{1,\Omega_\mathrm{f}}$
0	1.1e-4	3.0e-3	6.7e-4	1.1e-6	3.5e-5
1	2.7e-5	1.6e-3	3.2e-4	3.5e-7	2.0e-5
2	7.1e-6	8.4e-4	1.6e-4	9.0e-8	1.0e-5
3	1.8e-6	4.5e-4	8.5e-5	2.8e-8	5.6e-6

TABLE 1. Errors in L^2-norm ($\|\cdot\|_{0,\Omega_\mathrm{f}}$) and H^1-norm ($\|\cdot\|_{1,\Omega_\mathrm{f}}$) for several values of h.

3.2. **Approximation of the advection-diffusion problem.** Let $P^1_{\mathrm{Lag},h}$ be the space of Lagrange finite elements of degree one whose functions have null mean-value and periodicity properties on $\partial\Omega_\mathrm{ff}$. We seek for $\underline{\chi}_h \in (P^1_{\mathrm{Lag},h})^3$ such that $\forall \underline{\psi} \in (P^1_{\mathrm{Lag},h})^3$

$$\int_{\Omega_\mathrm{f}} \underline{\underline{\nabla}}\chi_h : \underline{\underline{\nabla}}\psi + \int_{\Omega_\mathrm{f}} (\underline{\underline{\nabla}}\chi \cdot (\pi_h \underline{u}_h)) \cdot \underline{\psi} = \int_{\Omega_\mathrm{f}} (\overline{\pi_h \underline{u}_h}^\mathrm{f} - \pi_h \underline{u}_h) \cdot \underline{\psi} + \int_{\partial\Omega_\mathrm{fs}} \underline{\psi} \cdot \underline{n} \qquad (6)$$

Since the field $\pi_h \underline{u}_h$ is conservative, problem (4) is well-posed. Let $\underline{\chi}$ be the solution of the continuous problem and $\underline{\chi}_h$ the solution of the discrete one. The following error estimate holds (Tardif d'Hamonville, Ern and Dormieux, 2006)

$$\|\underline{\chi}-\underline{\chi}_h\|_{0,\Omega_\mathrm{f}} + h\|\underline{\chi}-\underline{\chi}_h\|_{1,\Omega_\mathrm{f}} \leq ch^2,$$

where c depends on the exact solution $\underline{\chi}$ but is independent of h.

3.3. **Validation.** In order to validate the numerical procedure, we perform simulations of transport in a circular cylinder. In this case, there exists an analytical solution for the flow velocity $\underline{u}$ and for the vector field $\underline{\chi}$. Consider a cylinder with radius $a < 1$ and generatrix parallel to $\underline{e}_1$. The elementary cell Ω is a cube of side length 1 centered on the cylinder. If $\underline{\alpha} = -\underline{e}_1$ the solution reads

$$\underline{u} = \frac{1}{4}(a^2 - r^2)\underline{e}_1 \qquad p_1 = 0 \qquad \underline{\chi} = (-\frac{1}{64}r^4 + \frac{1}{32}a^2r^2 - \frac{1}{96}a^4)\underline{e}_1$$

where $r = \sqrt{z_2^2 + z_3^2}$ is the radial distance from the cylinder axis. All the coefficients of the diffusion and dispersion tensors vanish except

$$(D^\mathrm{hom}_\mathrm{diff})_{11} = \varphi \qquad \text{and} \qquad (D^\mathrm{hom}_\mathrm{disp})_{11} = \frac{1}{3072}\varphi a^6$$

where $\varphi = \pi a^2$ is the porosity.

This solution is compared with the numerical results obtained using the three-dimensional finite element method described above. Several quasi-uniform meshes characterized by the maximal mesh-size $h_i = h_0.2^{-i}$, $i \in [\![0, 3]\!]$, are tested. For each mesh the difference between analytical and numerical solutions is measured in various norms. Table 1 presents the convergence results. We observe that the convergence orders are in close agreement with theoretical predictions.

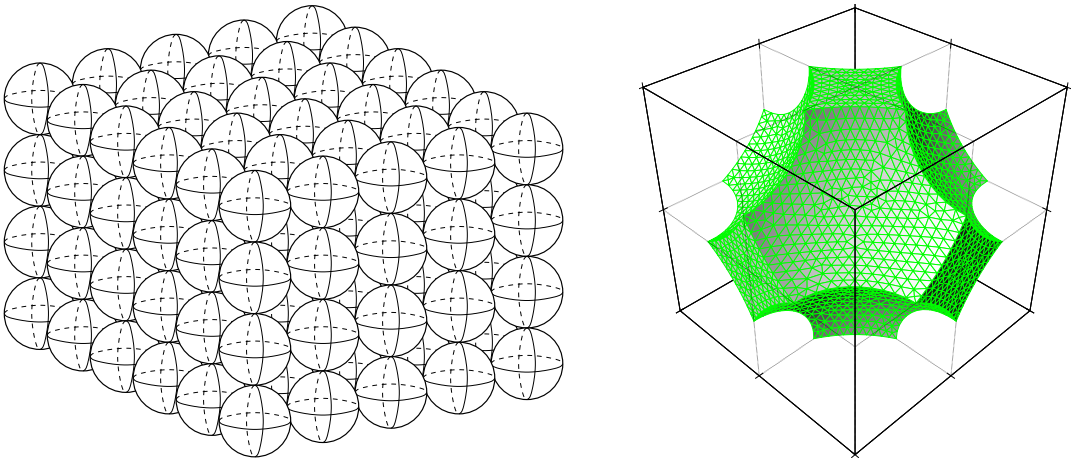

FIGURE 1. Example of a cubic network of spheres and mesh of Ω_f corresponding to such a network where the radius of the spheres is 0.57.

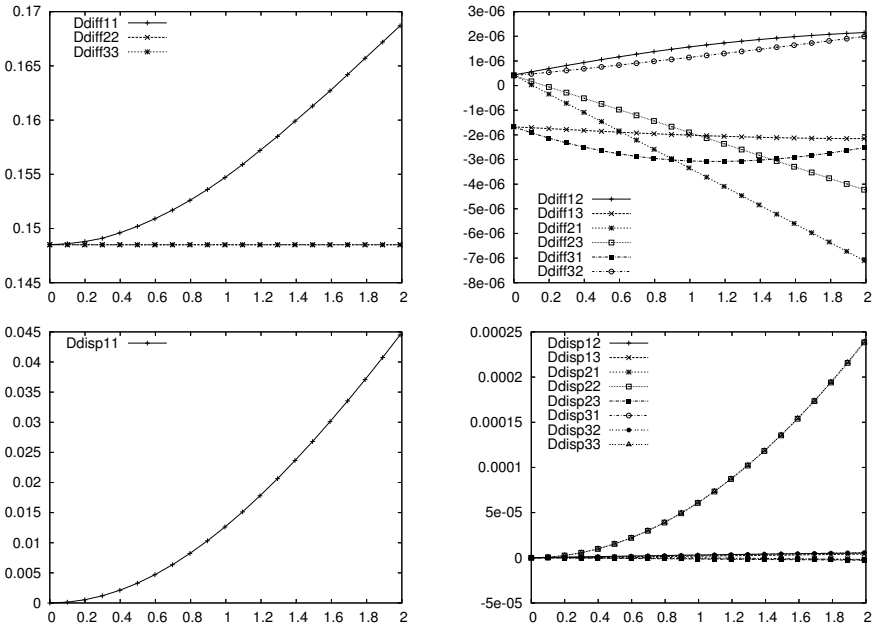

FIGURE 2. Evolution of the coefficients of the diffusion and dispersion tensors as a function of the mean velocity magnitude. Upper row : diffusion tensor. Lower row : dispersion tensor.

4. Results on sphere networks

4.1. **Influence of the velocity magnitude.** To investigate the influence of the velocity magnitude on the diffusion and dispersion tensors, we proceed as follows. First, a pore morphology is chosen and the flow velocity is computed for a macroscopic pressure gradient of magnitude equal to one. This yields the discrete velocity field $\underline{u}_h$. Then, in the

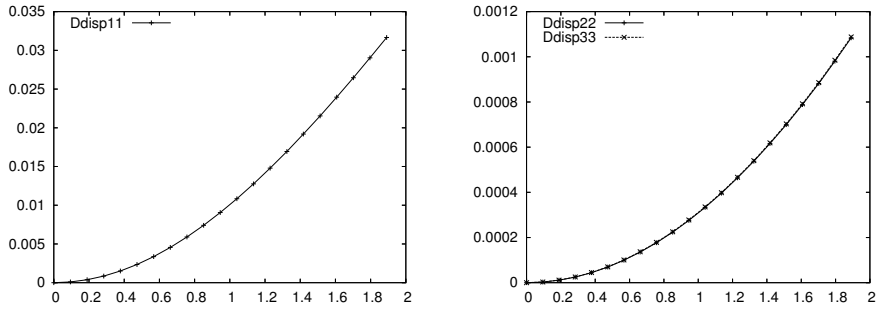

FIGURE 3. Diagonal coefficients of the dispersion tensor for the centered cubic network.

advection-diffusion problem, the velocity field is rescaled as $\underline{u}_h^\lambda = \lambda \underline{u}_h$ where the parameter λ varies up to $\frac{1}{\varsigma_{\Omega_f}}$ to respect the assumption of homogenizability made in the double scale expansion analysis.

Consider a cubic network of spheres with unit side length and sphere radius $r_s = 0.57$ (see Figure 1). The porosity associated with this morphology is $\varphi = 0.275$ and with a macroscopic pressure gradient oriented along $\underline{e}_1$, the numerical simulation of the flow yields $\varsigma_{\Omega_f} = 1.34\ 10^{-2}$. The computed permeability is $2\ 10^{-3}$. We perform numerical simulations of the advection-diffusion problem for the parameter λ varying between 0 and 1000 (which falls slightly beyond the strict validity limit based on $\frac{1}{\varsigma_{\Omega_f}}$). Figure 2 presents the values of the coefficients of the diffusion and dispersion tensors as a function of the mean velocity magnitude.

We observe that the extra-diagonal coefficients of the tensors are negligible, and that the longitudinal diffusion and both longitudinal and transversal dispersion grow non-linearly (close to quadratically) with respect to the velocity magnitude.

4.2. **Influence of the pore morphology.** Consider a similar elementary cell but with the parameter r_s now set to 0.56. A small sphere with radius $r_c = 0.15$ is added in the center of the cell. This morphology corresponds to a centered cubic network of spheres. The porosity associated with this morphology is $\varphi = 0.288$. A macroscopic pressure gradient oriented along $-\underline{e}_1$ is imposed which yields $\varsigma_{\Omega_f} = 1.14\ 10^{-2}$. The permeability is $1.9\ 10^{-3}$ which is close to the value of $2\ 10^{-3}$ obtained with the cubic sphere network in the previous section. We perform numerical simulations for λ varying between 0 and 1000. Figure 3 shows the evolution of the diagonal coefficients of the dispersion tensor as a function of the mean velocity magnitude.

Comparing with the previous results, we observe that the longitudinal dispersion is somewhat lower in the case of the centered cubic network, while the transversal dispersion is higher than the one in the cubic network by up to an order of magnitude. It can be explained by the higher tortuosity of the morphology in the centered cubic network which increases the mixing of the fluid.

5. CONCLUSION

The finite element tool designed in this work can be used to evaluate quantitatively diffusion and dispersion tensors in the presence of advection for various three-dimensional

pore morphologies. As such, it can be used as a pre-processing tool in the simulation of macroscopic transport in various applications.

References

J.-L. Auriault, (2005), Transport in porous media; upscaling by multiscale asymptotic expansions, Applied micromechanics of porous materials, CISM Courses and Lectures n. 480 (L. Dormieux and F.-J. Ulm, eds.), Springer, Wien, NewYork.

P. Bastian and B. Rivière, (2003), Superconvergence and $H(\mathrm{div})$ projection for discontinuous Galerkin methods, *Internat. J. Numer. Methods Fluids* ***42***, 1043–1057.

J. Bear and Y. Bachmat, (1990), *Introduction to modeling of transport phemomena in porous media*, Kluwer Academic Publishers.

F. Brezzi, J. Douglas Jr., and L. Marini, (1985), Two families of mixed finite elements for second order elliptic problems, *Numer. Math.* ***47***, 217–235.

L. Dormieux and E. Bourgeois, (2002), *Introduction à la micromécanique des milieux poreux*, Presses de l'ENPC, Paris.

H. Ene and E. Sanchez-Palencia, (1975), Equations et phénomenes de surface pour l'ecoulement dans un modele de milieu poreux, *Journal de Mécanique* ***14***, 73–108.

A. Ern and J.-L. Guermond, (2004), *Theory and practice of finite elements*, Applied Mathematical Sciences, vol. 159, Springer-Verlag, New York, NY.

E. Sanchez-Palencia, (1980), *Non-homogeneous media and vibration theory*, Lecture Notes in Physics, vol. 127, Springer-Verlag, Berlin-New York.

P. Tardif d'Hamonville, A. Ern, and L. Dormieux, (2006), Numerical evaluation of diffusive and dispersive transport in periodic porous media with advection, Preprint CERMICS, `http://cermics.enpc.fr/reports/CERMICS-2006/CERMICS-2006-297.pdf`.